Progress in Organic Coatings 67 (2010) 225–232

Contents lists available at ScienceDirect

Progress in Organic Coatings

journal homepage: www.elsevier.com/locate/porgcoat

Study of methoxyphenylquinoxalines (MOPQs) as photoinitiators in the negative photo-resist

Lida Sun, Xuesong Jiang*, Jie Yin

School of Chemistry and Chemical Technology, State Key Lab of Metal Matrix Composite, Shanghai Jiao Tong University, Shanghai 200240, People's Republic of China

ARTICLE INFO

Article history:
Received 29 September 2009
Received in revised form 5 December 2009
Accepted 12 December 2009

Keywords:
Photoinitiator
Quinoxalines
Negative photo-resist

ABSTRACT

To develop photoinitiator systems of high performance for the negative photo-resist, we synthesized six methoxyphenylquinoxalines (MOPQs) and investigated the photopolymerization of 2,2-bis(4-(acryloxypolyethoxy)phenyl)propane (A-BPE-10) initiated by these MOPQs in the negative photo-resist. MOPQs possess suitable UV–vis maximum absorption wavelengths in the range of 349–402 nm, along with high extinction coefficients ε. Except for T3MOP-DQ and T4MOP-DQ, the other four MOPQs, D3MOP-Q, D4MOP-Q, D3MOP-BenQ and D4MOP-BenQ, could initiate photopolymerization of A-BPE-10 in the negative photo-resist very efficiently. In particular, D3MOP-BenQ was the most efficient, with almost 100% final conversion in the presence of 2-mercaptobenzothiazole (MBO) as a coinitiator. Among the four coinitiators LCV, MBO, NPG and MDEA, MBO was the best coinitiator for MOPQs. The negative photo-resist containing MOPQs as a photoinitiator can also form good patterns on copper through photolithography. These characteristics make MOPQs potential photoinitiators in the negative photo-resist.

1. Introduction

As a simple and energy saving process of creating patterns on various substrates, the negative photo-resist is widely used in the fabrication of printed circuit boards (PCBs), which is one of the key materials in the modern electronics industry [1–7]. Usually, the negative photo-resist is comprised of the supporting polymer, crosslinker monomer and photoinitiator system. Photoinitiator systems can absorb light of a particular wavelength to generate active species, which can convert a crosslinker monomer into a crosslinked network in the negative photo-resist. Therefore, photoinitiator systems play a very important role in the negative photo-resist, and many efforts have been directed at the development of photoinitiator systems with high performance [8–10]. Among the most studied photoinitiator systems are those in which radicals are generated through bimolecular processes consisting of an excited chromophore and hydrogen donor as a coinitiator (hydrogen-abstraction photoinitiator system) [11–14].

Due to the excellent UV–vis absorption of dye chromophores, combinations of dyes with various hydrogen donors can provide a photoinitiator system with high performance for photopolymerization [15–17]. Quinoxaline possesses a structure similar to a dye, and can be expected to be a potential hydrogen-abstraction photoinitiator due to its tunable UV–vis absorption between 320 and 420 nm and its electron–acceptor moiety [18–21]. To the best of our knowledge, only a few studies on quinoxalines as photoinitiators have been reported. Arsu and coworkers investigated quinoxaline derivatives in UV-cured coatings [22], and Paczkowisky et al. studied a dye photoinitiator based on the indolo-quinoxaline skeleton [23].

As part of our continuous studies on the development of highly efficient photoinitiator systems for the negative photo-resist [24–27], a study of methoxyphenylquinoxaline derivatives (MOPQs) as photoinitiators in the negative photo-resist is presented. The methoxy group as a substituent on photoinitiator molecules is of our interest because it can not only enhance the solubility of the photoinitiator in the negative photo-resist, but also lead to a red-shift of the absorption of the electron-accepting photoinitiator. As is known, the most widely used commercial photoinitiator systems in the negative photo-resist are based on hexaarylbiimidazole (HABI) systems. The most widely used HABI derivatives, such as 2,2′-bis(2-chlorophenyl)-4,4′,5,5′-tetraphenyl-1,2′-biimidazole (BCIM), have been developed over about three decades. However, BCIM does not possess a satisfactory UV absorption, as its maximum absorption peak is below 300 nm. Moreover, BCIM has several drawbacks, such as having two chloride atoms in the molecule, relatively low solubility and forms sludge (precipitation) in the developing bath. Therefore, developing better photoinitiator systems with high performance for the negative photo-resist is a significant challenge. As dye molecules, quinoxalines possess suitable UV absorption properties with a tunable maximum absorption peak. To evaluate the possibil-

* Corresponding author. Tel.: +86 21 54747445; fax: +86 21 54747445.
E-mail addresses: ponygle@sjtu.edu.cn (X. Jiang), jyin@sjtu.edu.cn (J. Yin).

0300-9440/$ – see front matter © 2009 Elsevier B.V. All rights reserved.
doi:10.1016/j.porgcoat.2009.12.005

ity of quinoxalines as photoinitiators for the negative photo-resist, we synthesized six new methoxyphenylquinoxaline derivatives (MOPQs) and studied the photopolymerization of A-BPE-10 initiated by these MOPQs in the negative photo-resist by photo-DSC.

2. Experimental

2.1. Materials

3,3′-Dimethoxybenzil was obtained from Shanghai Sanshi science and technology Co. (Shanghai, China). 1,2-Diaminobenzene was provided by China National Pharmaceutical Group Co. (Shanghai, China). 3,3′,4,4′-Biphenyltetramine, 4,4′-dimethoxybenzil and leucocrystal violet (LCV) were purchased from Aldrich Chemical Company. 2-Mercaptobenzothiazole (MBO) was obtained from J and K Chemical Co. (Shanghai, China). 2,3-Diaminonaphthalene, N-phenylglycine (NPG) and N-methyldiethanolamine (MDEA) were purchased from Alfa Aesar. 2,2-Bis(4-(acryloxypolyethoxy)phenyl)propane (A-BPE-10) was provided by Shin-Nakamura Chemical Co., Ltd. Copoly(styrene-*co*-methylmethacrylate-*co*-methacrylic acid) (M_n = 94,000) was synthesized in our laboratory. Other chemicals were obtained from China National Pharmaceutical Group Co. (Shanghai, China). All reagents were used as received except as noted.

2.2. Synthesis of six methoxyphenylquinoxalines (MOPQs)

Six MOPQs were synthesized through a one-step reaction according to Scheme 1. The detailed experimental procedures for MOPQs are shown as follows.

2.2.1. Synthesis of 2,3-bis(3-methoxyphenyl)quinoxaline (D3MOP-Q)

4 mmol of 1,2-diaminobenzene and 4 mmol of 3,3′-dimethoxybenzil were dissolved in 25 mL of ethanol and stirred under nitrogen. The mixture was refluxed for 12 h, and was then poured into a 10-fold volume of petroleum ether. The precipitant was filtered and recrystallized from ethanol to furnish *D3MOP-Q*.

API-ES-LC/MS: *m*/*z* 343.0; $C_{22}H_{18}N_2O_2$ (342). Calcd. C 77.17, H 5.30, N 8.18. Found C 76.49, H 5.32, N 8.10. ^{1}H NMR (DMSO-d_6), δ (ppm): 3.63 (OCH_3); 6.94, 7.02, 7.03, 7.25, 7.85, 8.13 (CH Ar). ^{13}C NMR (DMSO-d_6), δ (ppm): 55.71 (OCH_3); 115.09, 115.77, 122.79, 129.82, 131.18, 140.70, 141.15, 159.51 (CH, C, Ar); 153.61 (C=N). FTIR (KBr): 1580 cm^{-1} (C=N).

2.2.2. Synthesis of 2,3-bis(4-methoxyphenyl)quinoxaline (D4MOP-Q)

4 mmol of 1,2-diaminobenzene and 4 mmol of 4,4′-dimethoxybenzil were dissolved in 25 mL of ethanol and stirred under nitrogen. The mixture was refluxed for 12 h, and was then poured into a 10-fold volume of petroleum ether. The precipitant was filtered and recrystallized from ethanol to furnish *D4MOP-Q*.

API-ES-LC/MS: *m*/*z* 343.0; $C_{22}H_{18}N_2O_2$ (342). Calcd. C 77.17, H 5.30, N 8.18. Found C 77.06, H 5.22, N 8.20. ^{1}H NMR (DMSO-d_6), δ (ppm): 3.77 (OCH_3); 6.92, 7.43, 7.81, 8.08 (CH Ar). ^{13}C NMR (DMSO-d_6), δ (ppm): 55.94 (OCH_3); 114.18, 129.36, 130.72, 131.86, 140.92, 160.41 (CH, C, Ar); 153.39 (C=N). FTIR (KBr): 1606 cm^{-1} (C=N).

2.2.3. Synthesis of 6-(2,3-bis(3-methoxyphenyl)quinoxalin-7-yl)-2,3-bis(3-methoxyphenyl) quinoxaline (T3MOP-DQ)

2 mmol of 3,3′,4,4′-biphenyltetramine, 4 mmol of 3,3′-dimethoxybenzil and 25 mL of 1,4-dioxane were added into a three-necked flask. The mixture was refluxed for 12 h, and was then poured into a 10-fold volume of petroleum ether. The precipitant was filtered and recrystallized from ethanol to furnish T3MOP-DQ.

MALDI: *m*/*z* 684.3; $C_{44}H_{34}N_4O_4$ (682). Calcd. C 77.40, H 5.02, N 8.21. Found C 77.39, H 5.00, N 8.25. ^{1}H NMR ($CDCl_3$), δ (ppm): 3.74 (OCH_3); 6.94, 7.12, 7.14, 7.27, 8.24, 8.33, 8.60 (CH Ar). ^{13}C NMR ($CDCl_3$), δ (ppm): 55.47 (OCH_3); 115.04, 115.60, 122.56, 127.69,

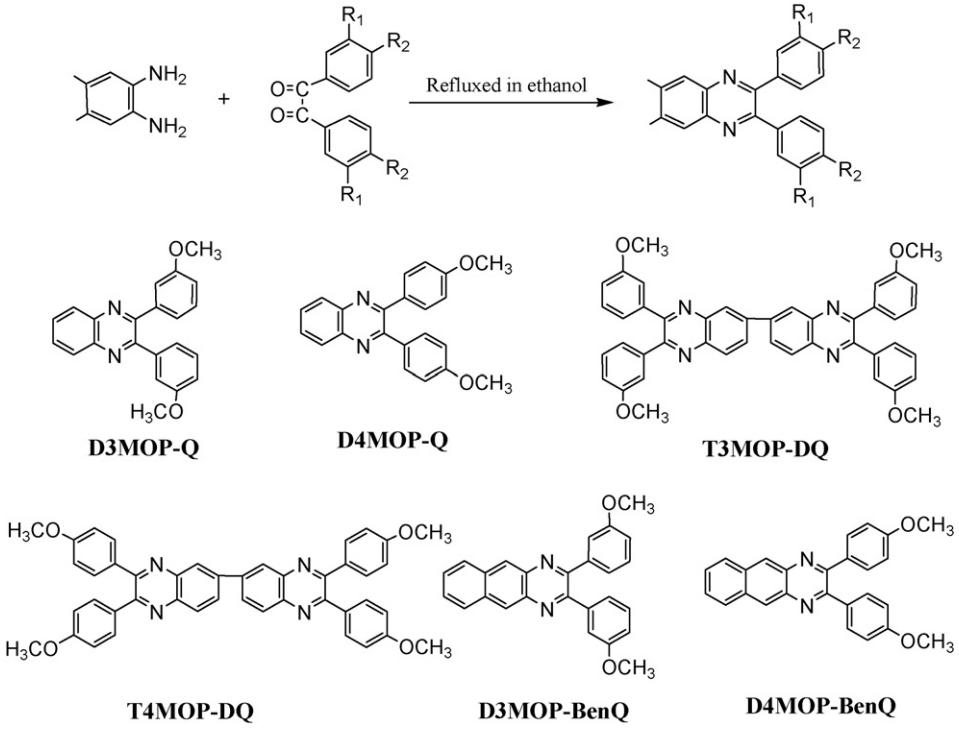

Scheme 1. Process for the synthesis of quinoxalines and their structures.

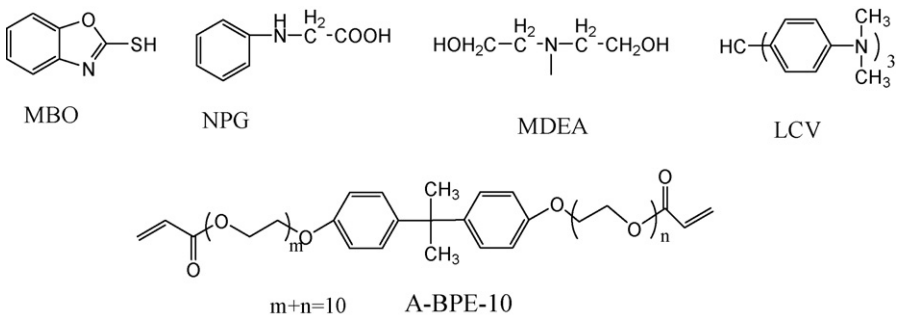

Scheme 2. Structures of coinitiators and the crosslinker.

129.77, 130.16, 140.46, 141.13, 141.47, 159.70 (CH, C, Ar); 153.82, 154.19 (C=N). FTIR (KBr): 1585 cm^{-1} (C=N).

2.2.4. Synthesis of 6-(2,3-bis(4-methoxyphenyl)quinoxalin-7-yl)-2,3-bis(4-methoxyphenyl) quinoxaline (T4MOP-DQ)

2 mmol of 3,3′,4,4′-biphenyltetramine, 4 mmol of 4,4′-dimethoxybenzil and 25 mL of 1,4-dioxane were added into a three-necked flask. The mixture was refluxed for 12 h, and was then poured into a 10-fold volume of petroleum ether. The precipitant was filtered and recrystallized from ethanol to furnish T4MOP-DQ.

MALDI: *m/z* 684.3; $C_{44}H_{34}N_4O_4$ (682). Calcd. C 77.40, H 5.02, N 8.21. Found C 76.80, H 4.98, N 8.08. ^{1}H NMR ($CDCl_3$), δ (ppm): 3.85 (OCH_3); 6.90, 7.54, 8.18, 8.25, 8.53 (CH Ar). ^{13}C NMR ($CDCl_3$), δ (ppm): 55.59 (OCH_3); 114.03, 127.52, 129.32, 129.99, 131.57, 141.23, 160.56 (CH, C, Ar); 153.37, 153.82 (C=N). FTIR (KBr): 1606 cm^{-1} (C=N).

2.2.5. Synthesis of 2,3-bis(3-methoxyphenyl)benzo[g]quinoxaline (D3MOP-BenQ)

4 mmol of 2,3-diaminonaphthalene and 4 mmol of 3,3′-dimethoxybenzil were dissolved in 1,4-dioxane. The mixture was refluxed for 12 h, and was then poured into a 10-fold volume of petroleum ether. The precipitant was filtered and recrystallized from ethanol to furnish *D3MOP-BenQ*.

API-ES-LC/MS: *m/z* 393.0; $C_{26}H_{20}N_2O_2$ (392). Calcd. C 79.57, H 5.14, N 7.14. Found C 78.33, H 5.06, N 6.67. ^{1}H NMR (DMSO-d_6), δ (ppm): 3.66 (OCH_3); 6.97, 7.06, 7.08, 7.28, 7.64, 8.25, 8.81 (CH Ar). ^{13}C NMR (DMSO-d_6), δ (ppm): 55.67 (OCH_3); 115.74, 122.70, 127.83, 129.17, 129.78, 134.30, 137.84, 140.89, 159.45 (CH, C, Ar); 154.33 (C=N). FTIR (KBr): 1592 cm^{-1} (C=N).

2.2.6. Synthesis of 2,3-bis(4-methoxyphenyl)benzo[g]quinoxaline (D4MOP-BenQ)

4 mmol of 2,3-diaminonaphthalene and 4 mmol of 4,4′-dimethoxybenzil were dissolved in 1,4-dioxane. The mixture was refluxed for 12 h, and was then poured into a 10-fold volume of petroleum ether. The precipitant was filtered and recrystallized from ethanol to furnish *D4MOP-BenQ*.

API-ES-LC/MS: *m/z* 393.0; $C_{26}H_{20}N_2O_2$ (392). Calcd. C 79.57, H 5.14, N 7.14. Found C 79.32, H 5.01, N 7.06. ^{1}H NMR ($CDCl_3$), δ (ppm): 3.85 (OCH_3); 6.90, 7.55, 8.09, 8.68 (CH Ar). ^{13}C NMR ($CDCl_3$), δ (ppm): 55.51 (OCH_3); 113.95, 126.74, 127.43, 128.74, 131.51, 134.13, 138.14, 160.61 (CH, C, Ar); 154.06 (C=N). FTIR (KBr): 1604 cm^{-1} (C=N).

2.3. Instruments

^{1}H and ^{13}C NMR spectra were recorded on a Varian Mercury Plus-400 nuclear magnetic resonance spectrometer (400 MHz) using $CDCl_3$ and DMSO-d_6 as solvents. FTIR spectra were recorded on a Perkin-Elmer Paragon 1000 spectrophotometer with KBr plates. Mass spectra were determined on an Agilent HP1100 LC/MSD mass spectrometer. Elemental analysis was carried out on an Elementar Vario EL III.

UV absorption spectra were recorded on an SHIMADZU UV-2550 UV–vis spectrophotometer. MOPQs were dissolved in chloroform at a concentration of 1×10^{-5} mol/L.

Fluorescence spectra were conducted on a Perkin-Elmer LS-50B spectrometer. MOPQs were dissolved in chloroform at a concentration of 4×10^{-7} mol/L. Fluorescence quantum yields (Φ_f) in chloroform were evaluated with respect to quinine bisulfate in 0.05 M aqueous sulfuric acid ($\Phi_f = 0.55$) [28–29].

2.4. Photodifferential scanning calorimetry (photo-DSC)

Photopolymerization of A-BPE-10 (Scheme 2) initiated by MOPQs in the negative photo-resist was carried out while acquiring photo-DSC measurements (DSC6200 Seiko Instrument) made with a high-pressure mercury lamp as the light source. Generally, the negative photo-resist was prepared by casting the photopolymer solution comprised of 2.5 g of crosslinker (A-BPE-10), 2.5 g of poly(styrene-*co*-methylmethacrylate-*co*-methacrylic acid) as the base copolymer, the photoinitiator system and 2 mL of 2-butanone on polyethylene terephthalate (PET) films, followed by drying in an oven. An approximately 1.3 mg film sample of 40 μm thickness was held in a sample cell for 1 min, and was then irradiated for 3 min on a photo-DSC with a 50 mW/cm^2 light intensity under a 50 mL/min nitrogen flow at 25 °C. The reaction heat is directly proportional to the amount of acrylate reacted in the system. By integrating the area under the exothermic peak, the conversion of the A-BPE-10 was determined according to Eq. (1) [30–31]:

$$C = \frac{\Delta H_t}{\Delta H_0^{theory}} \quad (1)$$

where ΔH_t is the reaction heat evolved at time t and ΔH_0^{theory} is the theoretical heat for complete conversion. $\Delta H_0^{theory} = 86$ kJ/mol [32] was used as the reaction heat of the acrylate double bond. The instantaneous rates of polymerization (Rp) were calculated according to the following equation [33–36]:

$$Rp = \frac{(dC/dt)(dH/dt)}{\Delta H_0} \quad (2)$$

2.5. Photolithography of the negative photo-resist

DFR samples were prepared using a procedure similar to the photo-DSC experiments. The photopolymer solution was prepared by mixing A-BPE-10 (2.5 g), poly(styrene-*co*-methylmethacrylate-*co*-methacrylic acid) (2.5 g), D4MOP-Q/LCV (0.025/0.05 mmol) and butanone (2 mL), followed by coating on PET film using a bar coater.

Table 1
UV–vis spectroscopic and fluorescent parameters of quinoxalines in chloroform.

Quinoxaline	Absorption				Fluorescence	
	λ_{max} (nm)	λ_{cutoff} (nm)	ε at λ_{max} (L mol^{-1} cm^{-1})	ε at 365 nm (L mol^{-1} cm^{-1})	λ_{em} (nm)	Φ
D3MOP-Q	349	393	10200	7900	454	0.0924
D4MOP-Q	369	415	14000	13800	433	0.2342
D3MOP-DQ	384	425	45000	33100	426	0.3329
D4MOP-DQ	400	444	51000	23900	444	0.4798
D3MOP-BenQ	389	448	10600	7200	460	0.0535
D4MOP-BenQ	402	457	18000	7600	456	0.6230

By drying in an oven at 110 °C for 15 min, 40 μm thick photopolymerizable DFR samples were prepared. The obtained DFR samples were laminated on a copper board (M-LAMINATOR, M4W-D) and then irradiated through a photo-mask by a high-pressure mercury lamp (CSUN UVE-M500). The exposed DFR was developed with Na_2CO_3 aqueous solution (TY-XY-5102), and the obtained pattern was observed by microscope (KEYENCE VF-7500 profile micrometer and scanning electron microscope HITACHI S-4800).

3. Results and discussion

3.1. Synthesis and photochemical properties of MOPQs

To investigate quinoxalines as photoinitiators in the negative photo-resist, six methoxyphenylquinoxaline derivatives (MOPQs) were synthesized according to Scheme 1. MOPQs can be synthesized through a one-step reaction between commercial diamines and benzils, and their structures were confirmed by FTIR and NMR spectroscopic analysis. The UV–vis spectra of the six obtained MOPQs are presented in Fig. 1, and detailed data of their photochemical properties are summarized in Table 1. According to Fig. 1 and Table 1, the maximal absorption wavelength (λ_{max}) of the six obtained MOPQs are in the range of 349–402 nm, with extinction coefficients (ε) above 1×10^4, which can be ascribed to the π–π^* absorption of the quinoxaline ring. The λ_{max} of MOPQs can be tuned by changing the molecular conjugation extent and position of the methoxy substituent. There is no doubt that an enhancement of the conjugation extent will lead to red-shifting of the λ_{max}. For example, the λ_{max} of D3MOP-DQ and D3MOP-BenQ red-shifts about 35–40 nm in comparison to D3MOP-Q. The position of the methoxy group also has a very obvious influence on the λ_{max}. As an electron-donating group, the methoxy group in the *p*-position of the phenyl ring causes a larger red-shift of λ_{max} than when it is in the *meta*-position, giving about a 15–20 nm red-shift of λ_{max}.

These satisfactory UV absorption properties make MOPQs potential photoinitiators because the irradiation wavelength of UV light most commonly utilized for photocuring is 365 nm. The fluorescence emission spectra of the six obtained MOPQs are shown in Fig. 2, and the detailed data of emission and fluorescence quantum yields (Φ_f) are summarized in Table 1. Except for D4MOP-BenQ, Φ_f for the other five MOPQs were less than 0.5. In the case of D3MOP-Q and D3MOP-BenQ, their Φ_f were very low, which may be ascribed to fast intersystem crossing (ic) from the singlet to triplet state.

3.2. Photopolymerization of A-BPE-10 initiated by MOPQs

The photo-DSC profiles of the photopolymerization of A-BPE-10 initiated by the MOPQs are presented in Fig. 3. The photopolymerization behavior appears to be similar to the other multifunctional crosslinkers [37–38]. The polymerization data are summarized in Table 2. In the presence of MBO as a coinitiator, D3MOP-Q, D4MOP-Q, D3MOP-BenQ and D4MOP-BenQ were efficient as photoinitiators in the negative photo-resist, and the final conversions of A-BPE-10 for these four MOPQs were higher than 85% according to Fig. 1 and Table 2. It should be noted that the final conversion for D3MOP-BenQ and D4MOP-BenQ were more than 90%; in the case of D3MOP-BenQ, 100% conversion could be achieved. This might be ascribed to the strong electron-accepting ability and excellent charge-transfer characteristics of the quinoxaline ring [18]. Under irradiation, MOPQ can abstract a hydrogen atom from the coinitiator MBO to generate active radicals through electron and proton transfer between the excited MOPQ and MBO. The strong electron-accepting ability and excellent charge-transfer characteristics of the quinoxaline ring promote hydrogen abstraction, resulting in the generation of enough radicals to efficiently initiate polymerization. Unlike the very obvious effects on UV–vis absorption, the position of the methoxy group in the MOPQ structure has no significant influence on the photoinitiating efficiency. The final conversion and

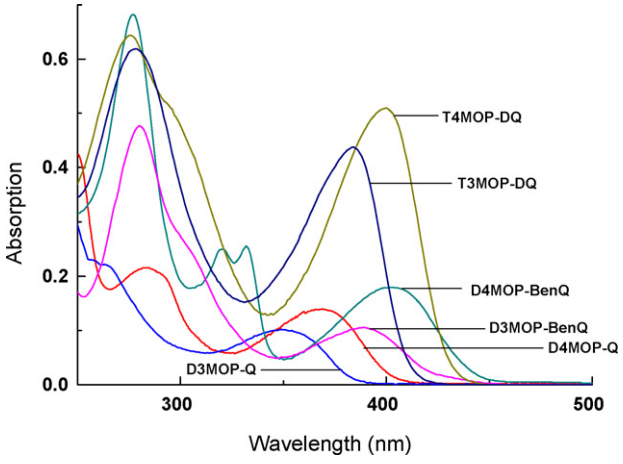

Fig. 1. UV–vis absorption spectra of six MOPQs in chloroform at a concentration of 1×10^{-5} mol/L.

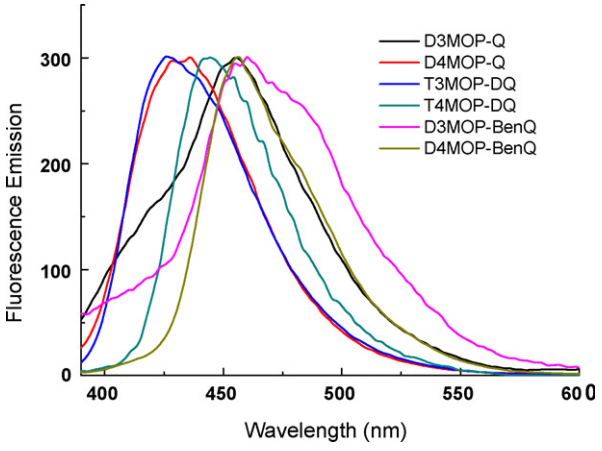

Fig. 2. Fluorescence emission spectra of six MOPQs in chloroform, normalized to the same intensity.

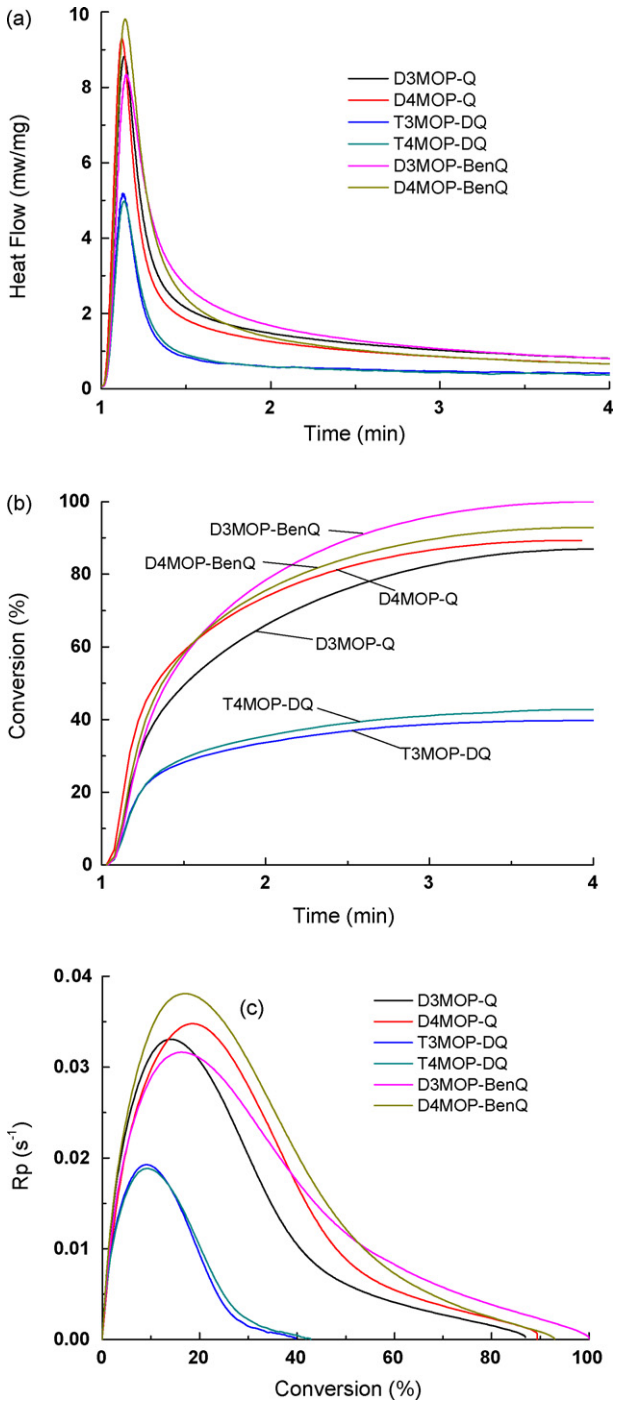

Fig. 3. Heat flow versus time curves of A-BPE-10 (a), conversion versus time curves of A-BPE-10 (b), Rp versus conversion curves of A-BPE-10 (c), initiated by the D3MOP-Q/MBO, D4MOP-Q/MBO, T3MOP-DQ/MBO, T4MOP-DQ/MBO, D3MOP-BenQ/MBO and D4MOP-BenQ/MBO systems, irradiated for 3 min at 25 °C with a 50 mW/cm^2 light intensity under a 50 mL/min nitrogen flow.

Table 2
Polymerization of A-BPE-10 initiated by six quinoxalines systems with MBO as the coinitiator, irradiated for 3 min at 25 °C with a 50 mW/cm^2 light intensity under a 50 mL/min nitrogen flow [quinoxalines] = 5 mmol/L.

Photoinitiators	ΔH (mJ/mg)	Conversion (%)	Rp_{max} ($\times 10^2$ (s^{-1}))	t_{Rpmax} (s)
D3MOP-Q	192.6	86.9	3.3	8.0
D4MOP-Q	198.0	89.4	3.5	7.3
T3MOP-DQ	88.0	39.7	1.9	7.7
T4MOP-DQ	94.9	42.8	1.9	8.0
D3MOP-BenQ	221.6	100.0	3.2	8.8
D4MOP-BenQ	205.9	92.9	3.8	8.4

Rp_{max} for D3MOP-Q were 86.9% and 3.3 s^{-1}, respectively, which were similar to those of D4MOP-Q. Compared with D3MOP-Q and D4MOP-Q, D3MOP-BenQ and D4MOP-BenQ were more efficient, which might be ascribed to their better UV absorption properties. Although T3MOP-DQ and T4MOP-DQ possess excellent UV absorption around 380–400 nm with high ε, they were not efficient in the photoinitiation of A-BPE-10, demonstrating final conversions of acrylate of less than 50%. This might be attributed to their low solubility and poor compatibility, which may be caused by their large, planar conjugated structures. Indeed, we found that T3MOP-DQ and T4MOP-DQ were difficult to disperse in the mixture of copolymer blend and A-BPE-10 when the negative photo-resist was prepared. In photocuring systems of high viscosity, chemical reactions such as photopolymerization of the crosslinker and hydrogen abstraction are controlled by diffusion. Therefore, the mobility of the photoinitiator and the generated radicals are the most important factors relating to the photopolymerization. Due to their larger structures, the mobilities of T3MOP-DQ and T4MOP-DQ are worse than those of the other four MOPQs, resulting in a lower photopolymerization rate and final conversion of A-BPE-10.

As one of the hydrogen abstraction (type II) photoinitiators, quinoxaline can be used as a photoinitiator in the presence of coinitiators such as amines and thiols. The quinoxaline molecules can be excited under the irradiation of UV light, followed by electron-transfer and hydrogen abstraction, which happen rapidly between excited photoinitiators and coinitiators, resulting in the formation of radicals produced from the quinoxaline molecules and other radicals derived from the coinitiators. Owing to the steric hindrance and delocalization of the unpaired electron, the radicals from quinoxalines are usually not active toward vinyl monomers. The photopolymerization of vinyl monomers is usually initiated by coinitiator radicals, which are rather active. The overall mechanism of the photoinitiation is shown in Scheme 3, from which we know that the quantity and activity of coinitiator radicals determine the photopolymerization rate. Therefore, the coinitiator plays an important role in quinoxaline photoinitiator systems. To find the best coinitiator for MOPQs, we investigated the photopolymerization of A-BPE-10 initiated by D4MOP-Q in the presence of four different coinitiators, LCV, MBO, NPG and DMEA (see Scheme 2). Fig. 4 presents photo-DSC profiles of the photopolymerization of A-BPE-10 initiated by D4MOP-Q in the presence of LCV, MBO, NPG and DMEA, and Table 3 summarizes the corresponding polymerization data. According to Fig. 4 and Table 2, MBO is the most efficient

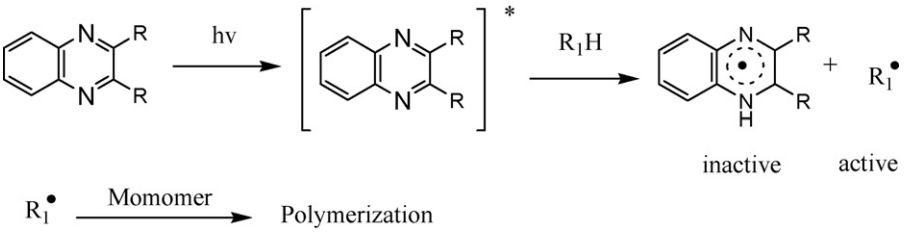

Scheme 3. Proposed mechanism for quinoxalines as photoinitiators.

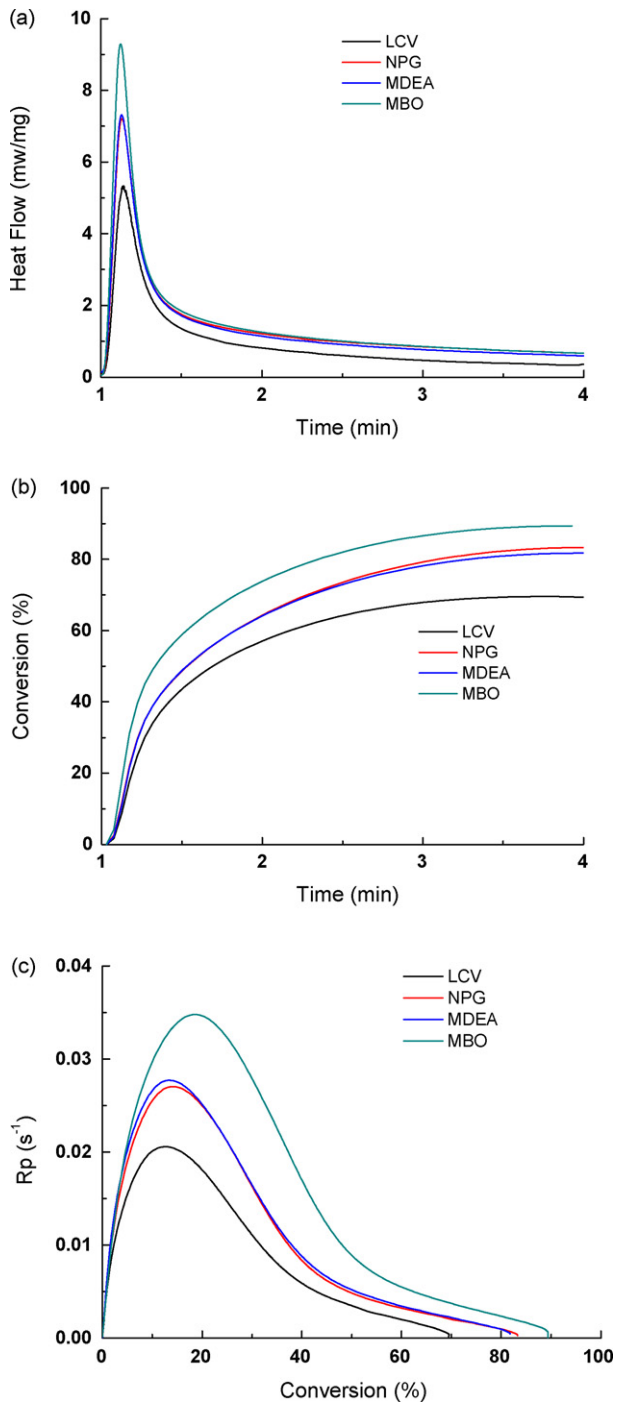

Fig. 4. Heat flow versus time curves of A-BPE-10 (a), conversion versus time curves of A-BPE-10 (b), Rp versus conversion curves of A-BPE-10 (c), initiated by the D4MOP-Q/LCV, D4MOP-Q/NPG, D4MOP-Q/MBO and D4MOP-Q/MDEA systems, irradiated for 3 min at 25 °C with a 50 mW/cm^2 light intensity under a 50 mL/min nitrogen flow.

Table 3
Photopolymerization of A-BPE-10 initiated by D4MOP-Q in the presence of the different coinitiators LCV, NPG, MBO and MDEA, irradiated for 3 min at 25 °C with a 50 mW/cm^2 light intensity under a 50 mL/min nitrogen flow [coinitiators] = 10 mmol/L.

Coinitiator	ΔH (mJ/mg)	Conversion (%)	Rp_{max} ($\times 10^2$ (s^{-1}))	t_{Rpmax} (s)
LCV	153.8	69.4	2.1	8.2
NPG	184.6	83.3	2.7	7.7
MBO	198.0	89.4	3.5	7.3
MDEA	181.2	81.8	2.8	7.7

among these four coinitiators, indicating that thiol can be used as an efficient coinitiator for MOPQs in the negative photo-resist.

Photoinitiator content is also important to photopolymerization in the negative photo-resist. Taking the D4MOP-Q/MBO system as an example, we further investigated the effect of quinoxaline concentration on photopolymerization in the negative photo-resist to find the most efficient concentration in the photoinitiator system. The concentration of the coinitiator MBO was kept constant. The photo-DSC profiles of the photopolymerization of A-BPE-10 initiated by D4MOP-Q/MBO at different concentrations are presented in Fig. 5, and the corresponding photopolymerization data are sum-

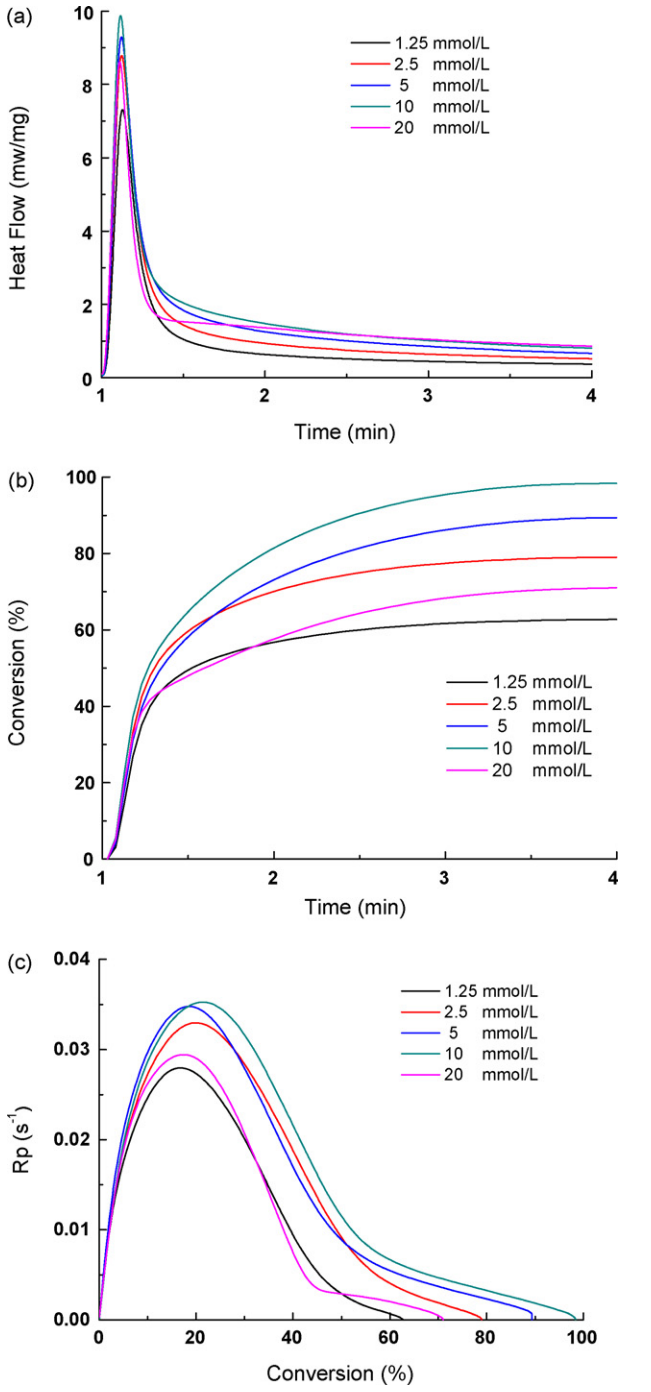

Fig. 5. Heat flow versus time curves of A-BPE-10 (a), conversion versus time curves of A-BPE-10 (b), Rp versus conversion curves of A-BPE-10 (c), initiated by different amounts of D4MOP-Q and 0.05 mmol MBO, irradiated for 3 min at 25 °C with a 50 mW/cm^2 light intensity under a 50 mL/min nitrogen flow.

Table 4
Photopolymerization of A-BPE-10 initiated by different amounts of D4MOP-Q in the presence of 0.05 mmol MBO as a coinitiator, irradiated for 3 min at 25 °C with a 50 mW/cm^2 light intensity under a 50 mL/min nitrogen flow.

Concentration of D4MOP-Q/mmol/L	ΔH (mJ/mg)	Conversion (%)	Rp_{max} ($\times 10^2$ (s^{-1}))	t_{Rpmax} (s)
1.25	139.0	62.7	2.8	7.7
2.5	175.0.	79.0	3.3	7.4
5	198.0	89.4	3.5	7.3
10	218.0	98.4	3.6	7.0
20	157.4	71.0	3.0	6.6

marized in Table 4. The Rp_{max} and the final conversion increased with an increase of photoinitiator concentration from 1.25 to 10 mmol/L, and decreased if more photoinitiator (20 mmol/L) was added. The highest Rp_{max} and the final conversion were achieved at a D4MOP-Q concentration of 10 mmol/L in our experiments. In the conventional UV photopolymerization, the polymerization rate and final conversion will increase with the increase of photoinitiator content due to the generation of more radicals. However, too much photoinitiator content will lead to a decrease of the photopolymerization rate and final conversion because of the "filter effect" [39]. The penetration of UV light decreases with the increase of depth. Too much D4MOP-Q content will prevent the UV light from penetrating into the lower layers of the negative photo-resist, consequently leading to incomplete photocuring of the crosslinkers, resulting in a decrease of Rp_{max} and final conversion.

3.3. Micro-pattern fabricated by the negative photo-resist

The photo- and SEM-images of a micro-pattern on copper fabricated by the negative photo-resist are shown in Fig. 6. D4MOP-Q was used as the photoinitiator and the exposure intensity of UV light was 30 mJ. The obtained micro-lines of the photo-resist exhibit a good shape, and the profile of the lines are steep, indicating that quinoxalines are potential photoinitiators in the negative photo-resist.

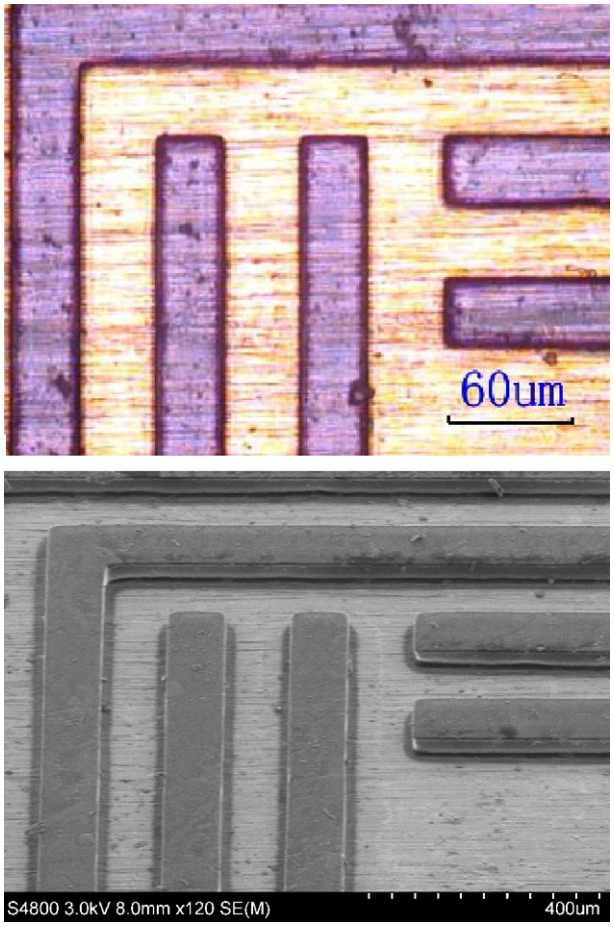

Fig. 6. Image of micro-pattern fabricated by DFR using D4MOP-Q as a photoinitiator: (A) photography and (B) SEM image.

4. Conclusion

We synthesized six methoxyphenylquinoxaline derivatives (MOPQs) and studied the photopolymerization of A-BPE-10 initiated by these MOPQs in the negative photo-resist. These MOPQs possessed good UV absorption properties. Among these six MOPQs, D3MOP-Q, D4MOP-Q, D3MOP-BenQ and D4MOP-Q were very efficient as photoinitiators, and MBO was the best coinitiator for MOPQs among the four coinitiators that we studied. In particular, D3MOP-BenQ could initiate the photopolymerization of A-BPE-10 in the negative photo-resist to a final conversion of almost 100%. These characteristics make MOPQs potentially valuable in the negative photo-resist.

Acknowledgment

We thank Mr. Kaji and Mr. Miyasaka from Hitachi-Chemical for discussions.

References

[1] T.S. Cheng, M.H. Wu, W.S. Weng, H. Chen, Mater. Lett. 57 (2002) 753.
[2] Y.K. Yang, T.C. Chang, Microelectron. Eng. 37 (2006) 746.
[3] K. Kojima, M. Ito, H. Morishita, N. Hayashi, Chem. Mater. 10 (1998) 3429.
[4] X. Allonas, J.P. Fouassier, H. Obeid, M. Kaji, Y. Ichihashi, J. Photopolym. Sci. Technol. 17 (2004) 35.
[5] P.W. Leech, N. Wu, Y. Zhu, J. Micromech. Microeng. 19 (2009) 065019.
[6] L.T. Jiang, T.C. Huang, C.Y. Chang, et al., J. Micromech. Microeng. 18 (2008) 015004.
[7] K. Stephan, N. Ouaini, R. Ferrigno, et al., J. Micromech. Microeng. 17 (2007) N69.
[8] B.M. Monroe, G.C. Weed, Chem. Rev. 93 (1993) 435.
[9] M. Kaji, Y. Muramatsu, Y. Nishimura, T. Arai, J. Photopolym. Sci. Technol. 20 (2007) 265.
[10] H. Igarashi, T. Igarashi, M. Sagawa, Y. Katsumura, T. Yamashita, et al., J. Photopolym. Sci. Technol. 20 (2007) 757.
[11] S.P. Pappas, UV Curing Science and Technology, Technology Marketting Corp., Norwalk, CT, 1978.
[12] X.S. Jiang, H.J. Xu, J. Yin, Polymer 45 (2004) 133.
[13] J.P. Fouassier, D.J. Lougnot, L. Avar, Polymer 36 (1995) 5005.
[14] T. Corrales, F. Catalina, C. Peinado, N.S. Allen, A.M. Rufs, C. Bueno, et al., Polymer 43 (2002) 4591.
[15] L. Vurth, P. Baldeck, O. Stephan, G. Vitrant, Appl. Phys. Lett. 92 (2008) 171103–171111.
[16] J. Kabatc, M. Kaczorowska, B. Jedrzejewska, J. Paczkowski, Appl. Phys. Lett. 108 (2008) 1636.
[17] M.V. Encinas, A.M. Rufs, S.G. Bertolotti, C.M. Previtali, Polymer 50 (2009) 2762.
[18] N. Arsu, M. Aydin, Angew. Makromol. Chem. 270 (1999) 1.
[19] M. Aydin, N. Arsu, Prog. Org. Coat. 56 (2006) 338.
[20] D. Braun, G. Quarg, Angew. Makromol. Chem. 43 (1975) 125.
[21] D. Braun, Angew. Makromol. Chem. 183 (1990) 17.
[22] D.K. Balta, S. Keskin, F. Karasu, N. Arsu, Polymer 60 (2007) 207.
[23] J. Paczkowski, et al., Polymer 45 (2004) 2559.
[24] Y.T. Shi, B.H. Wang, X.S. Jiang, J. Yin, M. Kaji, H. Yori, J. Appl. Polym. Sci. 105 (2007) 2027.
[25] Y.T. Shi, J. Yin, M. Kaji, H. Yori, Polym. Eng. Sci. 46 (2006) 474.
[26] Y.T. Shi, J. Yin, M. Kaji, H. Yori, Polym. Int. 55 (2006) 330.
[27] X.S. Jiang, J. Yin, Y. Murakami, M. Kaji, J. Photopolym. Technol. 22 (2009) 351.
[28] Wang, U.S. Pat. 7,261,996 (2007).

[29] C.A. Parker, W.T. Rees, Analyst 85 (1960) 587.
[30] G.Z. Chen, X.Z. Huang, Z.Z. Zheng, et al., Fluorescence Analytical Methods, Science Press, Beijing, 1990.
[31] X.S. Jiang, J. Yin, Macromolecules 37 (2004) 7850.
[32] E. Andrzejewska, Prog. Polym. Sci. 26 (2001) 605.
[33] E. Andrzejewska, Polymer 37 (1996) 1039.
[34] M. Wen, V. Alon, Mccormick, Macromolecules 33 (2000) 9247.
[35] I.V. Khudyakov, J.C. Legg, M.B. Purvis, Ind. Eng. Chem. Res. 38 (1999) 3353.
[36] T.F. Scott, et al., Polymer 44 (2003) 671.
[37] J. Wei, H.Y. Wang, X.S. Jiang, J. Yin, Macromolecules 40 (2007) 2344.
[38] Y.N. Wen, X.S. Jiang, J. Yin, Prog. Org. Coat. 66 (2009) 65.
[39] S.H. Zhang, Q.X. Zhou, et al., Polymer 42 (2001) 7575.